World Journal of
Biological and Pharmaceutical Research

Journal homepage: https://zealjournals.com/wjbpr/

ISSN: 2799-0338 (Online)

(RESEARCH ARTICLE)

Check for updates

Identification of infectious disease spatial clusters based on local Moran's I statistic: A case study of dengue hemorrhagic fever

Thi-Tuyet-Mai Nguyen [1,*], Thi-Quynh Nguyen [2] and Thi-Hien Cao [2]

[1] *Faculty of Pharmacy, East Asia University of Technology, Hanoi, Vietnam.*
[2] *Faculty of Nursing, East Asia University of Technology, Hanoi, Vietnam.*

World Journal of Biological and Pharmaceutical Research, 2023, 05(02), 038–048

Publication history: Received on 18 November 2023; revised on 24 December 2023; accepted on 27 December 2023

Article DOI: https://doi.org/10.53346/wjbpr.2023.5.2.0075

Abstract

Background: One of the most prevalent tropical illnesses that impact people is dengue. Dengue and dengue hemorrhagic fever (DF/DHF) have become much more common within the past few decades. The purpose of this study is to use the local Moran's I statistic to identify any spatial clustering of dengue hemorrhagic fever in Ho Chi Minh City, Vietnam, during the months of June through July of 2023.

Methods: The data distribution was first examined using descriptive statistics. The spatial clustering of dengue hemorrhagic fever over these four months was then examined using the global Moran's I statistic, Moran's I scatterplot, and local Moran's I statistic. More precisely, using the local Moran's I statistic, dengue hemorrhagic fever clusters (high-high and low-low) and geographical outliers (low-high and high-low) were found in Ho Chi Minh City.

Results: It was discovered that DHF infection rates in Ho Chi Minh City likely to rise gradually between June and July of 2023. High-high spatial clustering of DHF infection rates was primarily found in urban areas and the city centre, despite the fact that this pattern has rapidly changed.

Conclusions: The results of this investigation showed that Ho Chi Minh City has statistically significant spatial clusters of DHF. The findings of this investigation further show that local Moran's I statistic is validated in the context of studying the spatial clustering of infectious diseases in general and DHF in particular. The research findings offer valuable insights into the knowledge of the dissemination of DHF.

Keywords: Infectious Disease; Spatial Clusters; Dengue Hemorrhagic Fever; Local Moran's I Statistic

1. Introduction

Any of the four dengue serotypes can cause dengue, an endemo-epidemic viral disease spread by mosquitoes. With Aedes aegypti serving as the primary vector, it is currently the most significant arthropod-borne viral illness in terms of morbidity and mortality (1). In recent decades, dengue has grown to be a serious global public health issue. Globally, dengue is the most common arboviral illness in humans. Four antigenically similar serotypes of Dengue viruses (DENV) co-circulate as members of the genus Flavivirus and family Flaviviridae (DENV-1, −2, −3, and −4) (2). Dengue hemorrhagic, dengue hemorrhagic fever (DHF), and the most serious and potentially lethal dengue shock syndrome are among the clinical symptoms of dengue (3). Dengue and dengue hemorrhagic fever (DF/DHF) have become much more common within the past few decades. Currently, over 100 nations have recognised dengue, and 2.5 billion people reside in dengue-prone areas. Globally, there are an estimated 50–100 million cases of DF and 250–500 000 cases of DHF per year (1). When female Aedes mosquitoes, such as Aedes albopictus and Aedes aegypti, bite humans, they can transmit

* Corresponding author: Thi-Tuyet-Mai Nguyen

the dengue virus. There is a higher chance of serious consequences following infection with a certain serotype of DENVs (4).

A crucial tool for analysing the spatial pattern of spatial objects is a spatial statistic. (5). In accordance with Tobler's First Law of Geography, epidemiological research have effectively used commonly used statistics for spatial auto-correlation analysis, such as global spatial statistics (Moran's I, Getis-Ord G* and Geary's C) and local indicators of spatial association (LISA) (6–9) in general, and in the investigation of COVID-19's transmission (10–12) and hand-foot-and-mouth disease (13,14) in particular. In keeping with this notion, popular statistics for geographical auto-correlation analysis, including global spatial statistics, have been effectively applied in infectious disease epidemiological studies (6–9) like the hand, foot, and mouth disease and COVID-19. For instance, the research of COVID-19 dissemination has made extensive use of these spatial information (10–12). More specifically, a study on spatial analysis and hotspots identification of COVID-19 utilising GIS (March and April, 2020) was successfully completed using spatial statistics (15) whereas Anselin local Moran's I indices and hot spot analysis were subsequently used to precisely identify high- and low-risk COVID-19 clusters worldwide. The locations of (visited) COVID-19 cases, for example, have been demonstrated most recently to be among the various COVID-19-related data that may be regarded as a form of spatial object with a spatial dimension that can be mapped using a GIS (5). Thus, spatial COVID-19 dispersed over Oman was also effectively evaluated with the aid of GIS approaches (16) whereas five geospatial methods were used in the assessment inside a GIS framework: a weighted mean centre, standard deviational ellipses, Moran's I autocorrelation coefficient, Getis-Ord General-G high/low clustering, and Getis-Ord G* statistic were used to examine the spatiotemporal distribution of COVID-19 in Oman (16). Furthermore, numerous efforts have been made to employ spatial statistics in research on the transmission of hand, foot, and mouth disease. For example, it was effective to determine the spatiotemporal distribution and hotspots of hand, foot, mouth disease (HFMD) in northern Thailand (17). In China, between 2008 and 2011, spatial clustering and a shifting trend in hand-foot-mouth disease were discovered (18). In Qinghai Province, China, LISA was effectively used from 2009 to 2015 to look at the epidemiological characteristics and geographic clusters of hand, foot, and mouth disease (19). Furthermore, utilising data from 2008 to 2011 at the provincial and county/district levels in China, exploratory spatial data analysis (ESDA) was utilised to perform spatial statistical analyses on geographical clustering and changing trend of the HFMD (18). Recently, the phenomena of HFMD outbreaks in Thai Land from 2003 to 2012 has been successfully explained by general statistics and spatial-temporal analysis using a GIS-based method (17). From 2008 to 2012, mainland China's counties' spatiotemporal cluster patterns of HFMD were examined using both local and global spatial autocorrelation analysis (20). In light of the findings from the COVID-19 and hand, foot, and mouth disease investigations, spatial statistics will be used in this study to investigate the spatial clustering of dengue hemorrhagic fever.

This study's objective is to examine the spatial clustering of dengue hemorrhagic fever in Ho Chi Minh City, Vietnam, from June to July of 2023. We will use the global, scatterplot, and local versions of the Moran's I statistic to identify spatial clustering of dengue hemorrhagic fever throughout these four months. More specifically, using the local Moran's I statistic, dengue hemorrhagic fever clusters (high-high and low-low) and geographical outliers (low-high and high-low) will be found in Ho Chi Minh City.

2. Materials and methods

2.1. Materials

In Vietnam, dengue hemorrhagic fever is still a dangerously new arboviral illness. DHF is endemic in Vietnam, with an estimated 1.6 million cases occurring annually in urban and periurban areas (21). Previous studies have shown that all four DENV serotypes had circulated in Vietnam at some point, with DENV-1 and DENV-2 being the most often detected serotypes, as is normal in hyperendemic nations (22). The dengue virus poses a major threat to public health around the globe. Ho Chi Minh metropolis, the largest metropolis in Vietnam, saw its largest DENV outbreak in over a decade. Significant morbidity and mortality result from it in hyperendemic countries like Vietnam (23). According to reports, DENV-1 was the most common serotype in Ho Chi Minh City and the surrounding areas until 2018 (23). A significant DENV outbreak in 2022 was in Ho Chi Minh City. The Ho Chi Minh Centre for Disease Control (HCDC) reported 78,561 dengue cases there. As a result, the analysis of the spatial clustering of DHF in Ho Chi Minh City was the main objective of this investigation.

Analysis of the spatial clustering of DHF incidence in Ho Chi Minh City was conducted using a dataset of DHF incidence that was gathered between June and September of 2023. The HCMC Centre for Disease Control (HCDC) website provided data on DHF incidence throughout these months. High DHF prevalence was found in Ho Chi Minh City's metropolitan areas, while low and extremely low DHF incidence was found in the suburbs to the north and south of the city.

2.2. Methods

2.2.1. Descriptive statistics

Summaries of the sample or population data are given via descriptive statistics. The field of descriptive statistics is characterised by the application of specific quantitative techniques to provide an overview of a sample's features. It is beneficial to offer clear and concise descriptions of the observations and the sample using statistics such as variance, mean, median, and charts. Data with a single variable are described using univariate descriptive statistics. Simply put, descriptive statistics are the numerical or graphical methods used to arrange and characterise the elements or properties of a particular sample (24). Descriptive statistics are primarily used to characterise the middle of a score distribution, also known as the measure of central tendency, and the score distribution known as the dispersion or variance (24). Descriptive statistics are also concise informational coefficients that provide an overview of a certain data collection, which may be a sample of the population or a representation of the complete population. By outlining the correlation between the variables in a sample or population, descriptive statistics help organise and summarise data (25). Measurements of central tendency and measurements of variability (spread) are the two categories into which descriptive statistics fall. Nominal, ordinal, interval, and ratio variables are among the types of variables included in descriptive statistics, along with measures of frequency, central tendency, dispersion or variation, and location (25). The standard deviation, variance, minimum and maximum variables, kurtosis, and skewness are measurements of variability, whereas the mean, median, and mode are measures of central tendency. The mean and median have been the most often utilised metrics among them in numerous quantitative research projects (26,27). Commonly used descriptive statistics, like the mean and median, were used in this work to calculate the local Moran's I statistic and quantify the central tendency of DHF incidence. Measures of centre, such as the mean, median, and mode, are the most well-known categories of descriptive statistics and are applied to practically every level of mathematics and statistics. One way to think about the median for a set of numerical data is as the middle number. The central observation that results from sorting the data in ascending order is called the median. By adding up each figure in the data set and dividing the result by the total number of figures in the collection, one can determine the mean, or average. Summing together all of the data values and dividing the result by the total number yields the arithmetic mean. Usually referred to as the mean or average, it is determined by the following formula:

$$x = \frac{1}{n}\sum_{i=1}^{n} x_i \text{.....(1)}$$

The sample standard deviation (SDEV), when derived from a population sample, quantifies the degree to which the sample data deviates from the sample mean. The variance's positive square root is the standard deviation. Compared to variance, standard deviation is a more useful tool for analysing variability in a data collection. The formula is used to calculate it:

$$SDEV = \sqrt{\frac{1}{n-1}\sum_{i=1}^{n}(x_i - \bar{x})^2} \text{.....(2)}$$

The statistical dispersion, or the spread of the data, is measured by the interquartile range (IQR). Other names for the IQR include the middle 50%, H spread, fourth spread, and midspread. It is described as the variation in the data's 75th and 25th percentiles. It is provided by Q3−Q1, in which:

$$Q_1 = \frac{(n+1)^{th}}{4} \text{.....(3)}$$

$$Q_3 = \frac{3(n+1)^{th}}{4} \text{.....(4)}$$

Since the IQR calculates the range of the middle half of the data, extreme observations have less of an impact on it. The spread of the middle half of the data distribution is shown by the interquartile range.

2.2.2. Global Moran's I statistic

The global Moran's I indicates whether spatial autocorrelation is present overall or not. In order to determine the global spatial clustering of dengue hemorrhagic fever incidence, this study used the global Moran's I statistic (28,29). Equation represents the definition of the global Moran's I statistic (4):

$$I = \frac{n}{S_0}\frac{\sum_{i=1}^{n}\sum_{j=1}^{n} W_{ij}(x_i-\bar{x})(x_j-\bar{x})}{\sum_{i=1}^{n}\sum_{j=\mathrm{i}}^{n} W_{ij}\sum_{i=1}^{n}(x_i-\bar{x})^2} \text{.....(5)}$$

where x_i and x_j are the dengue hemorrhagic fever incidence for district *i* and district *j*; $\bar{x}$ is the mean of the dengue hemorrhagic fever incidence and be given by $\bar{x} = \sum_{i=1}^{n} \frac{x_i}{n}$; *n* is the total number of districts in the whole study area; and W_{ij} is a $(n \times n)$ spatial weight matrix (30).

The global Moran's I coefficient values are in the interval [-1, +1] (30). When there is positive geographic autocorrelation in the data, global Moran's I values are positive; conversely, when there is negative spatial autocorrelation, global Moran's I values are negative (31). The DHF distribution shows no signs of randomness or regional autocorrelation when global Moran's I coefficient values are near zero.

2.2.3. Local Moran's I statistic

Since the local Moran's I statistic is one of the LISA statistics that is most frequently employed in research, this study used it to measure the spatial clustering of low and high dengue hemorrhagic fever incidence in each district (30). The following formula provides the local Moran's I statistic (I_i) of dengue hemorrhagic fever incidence at district i (32):

$$I_i = \frac{(x_i - \bar{x})}{\sigma^2} \sum_{j\#i, j \in J_i}^{N} W_{ij}(x_j - \bar{x}) \text{.....(6)}$$

where x_i, x_j, $\bar{x}$, and W_{ij} are defined in equation (1); *N* is the total number of neighborhood districts (30); J_i denotes the neighborhood set of dengue hemorrhagic fever incidence at district *i*; $j\#i$ implies that the sum of all $(x_j - \bar{x})$ of nearby neighbourhood districts of district *i* but not including x_j; and σ^2 is the variance of *x*, given in equation (3). W_{ij} defines neighbor connectivity and can be constructed using first or second order of contiguity (Figure 2).

$$\sigma^2 = \frac{1}{N} \sum_{j=1}^{N} (x_i - \bar{x}) \text{.....(7)}$$

If I_i follows a normal distribution, the statistical significance of Moran's I statistic can be examined, and the Z-scores can be ascertained as follows:

$$Z_{I_i} = -\frac{I_i - E(I_i)}{\sqrt{Var(I_i)}} \text{.....(8)}$$

where: E(I_i) and Var(I_i) are the arithmetic expectation and variance of the Moran statistic at district i, respectively, and are expressed using by the following equations::

$$E(I_i) = -\frac{w_i}{n-1} \text{.....(9)}$$

$$Var(I_i) = E(I_i^2) - [E(I_i)]^2 = \frac{w_{i(2)}(n-b_2)}{n-1} + \frac{2w_{i(kh)}(2b_2-n)}{(n-1)(n-2)} + \frac{{w_i}^2}{(n-1)^2} \text{.....(10)}$$

with:

$$E(I_i) = -\frac{w_i}{n-1} \text{.....(11)}$$

$$Var(I_i) = E(I_i^2) - [E(I_i)]^2 = \frac{w_{i(2)}(n-b_2)}{n-1} + \frac{2w_{i(kh)}(2b_2-n)}{(n-1)(n-2)} + \frac{{w_i}^2}{(n-1)^2} \text{.....(12)}$$

$$w_i = \sum_{j=1}^{n} w_{ij}(d) \text{.....(13)}$$

$$b_2 = \left[\frac{1}{n}\sum_{i=1}^{n}(x_i - \bar{x})^4\right]\left[\frac{1}{n}\sum_{i=1}^{n}(x_i - \bar{x})^2\right]^{-2} \text{.....(14)}$$

$$w_{i(2)} = \sum_{j=1}^{n} w_{ij}(d)^2 \text{.....(15)}$$

$$2w_{i(kh)} = \sum_{\substack{k=1 \\ k\neq i}}^{n} \sum_{\substack{h=1 \\ h\neq i}}^{n} w_{ik}(d) w_{ih}(d) \text{.....(16)}$$

It can be seen that the level of spatial clustering of dengue hemorrhagic fever incidence at each district is indicated by local Moran's I statistic. Similar to the global Moran's I statistic, the local Moran's I value at district i (I_i) also ranges between -1 and +1 (30). A high positive I_i shows the district i has a similarly high or low number of dengue hemorrhagic fever incidence cases as its neighbors and called the ''spatial cluster''(31).

3. Results and discussions

3.1. Spatial distribution of DHF incidence

Table 1 provided a summary of the DHF infection rates per 100,000 persons. The boxplots in Figure 1 and the maps in Figure 2 displayed the distribution of DHF incidencet. According to data in Table 1, the average monthly increase in the number of DHF cases (or DHF infection rate) has been between 8.4 and 11.9, on average. Month by month, the DHF incidence dispersion also rose, with corresponding IQR and SDEV values of 4 and 6, and 4.1 and 5.7, respectively. The majority of districts had low DHF infection rates (median is smaller than mean), according to data from the boxplots in Figure 2. In the meantime, data from the boxplots in Figures 2-a and b revealed that most districts had a high rate of DHF infections (median is higher than the average value). Consequently, it is evident that from June to July of 2023, the city's DHF infection rate tends to rise gradually.

Table 1 Statistical descriptives for dengue hemorrhagic fever

Time periods	Statistical descriptives							
	Min	Mean	Median	Max	Q1	Q3	IQR	SDEV
June	0	8.4	8	20	8	12	4	4.1
July	3	11.9	11.5	28	8	14	6	5.7

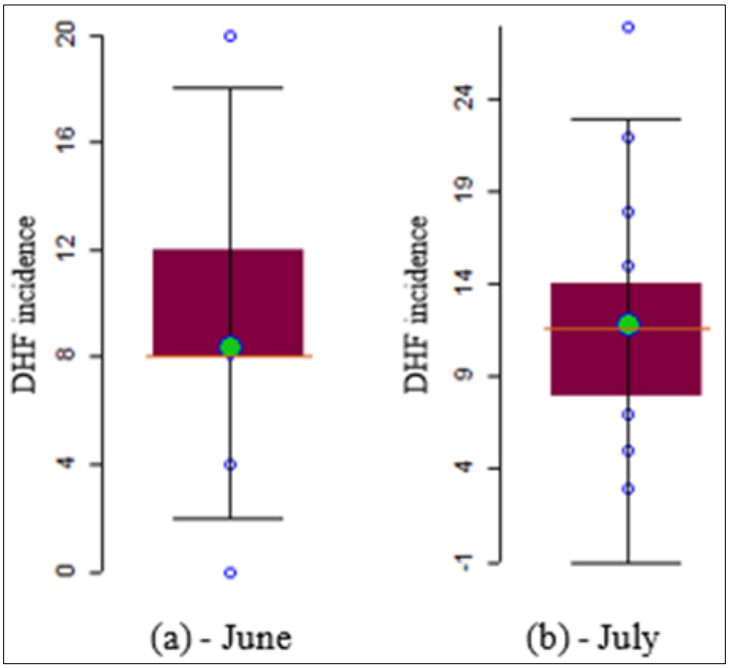

Figure 1 Boxplots of dengue hemorrhagic fever incidence

Figure 2's data indicates that while low DHF infection rates were found in suburban areas to the north and south of the city, high DHF infection rates were primarily found in the city's central districts. Specifically, there was a trend towards an increase in infection rates over time in metropolitan areas. High infection rates in June were mostly found in the city's west. Consequently, it is evident that the areas with high DHF infection rates underwent constant alteration.

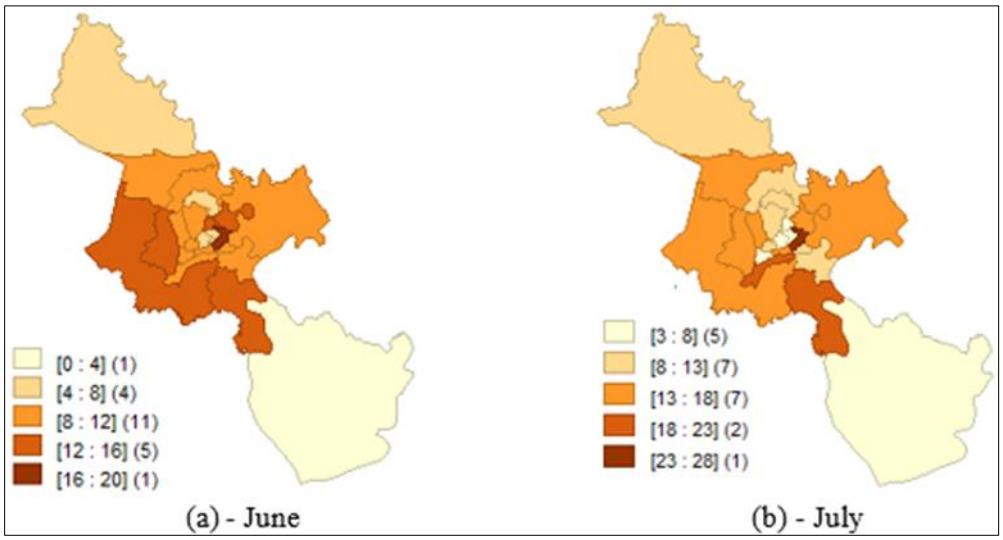

Figure 2 Equal intervals maps of dengue hemorrhagic fever incidence

3.2. Moran's I scatterplot

The degree of globally geographic autocorrelation of dengue hemorrhagic fever in June and July of 2023 is depicted by data from Moran scatter plots in Figure 3. In these months, the global Moran's I statistic yielded values of -0.13 and -0.23, respectively. Overall, there was negative autocorrelation between the DHF infection rates in these districts over the course of four months, as indicated by the negative global Moran values.

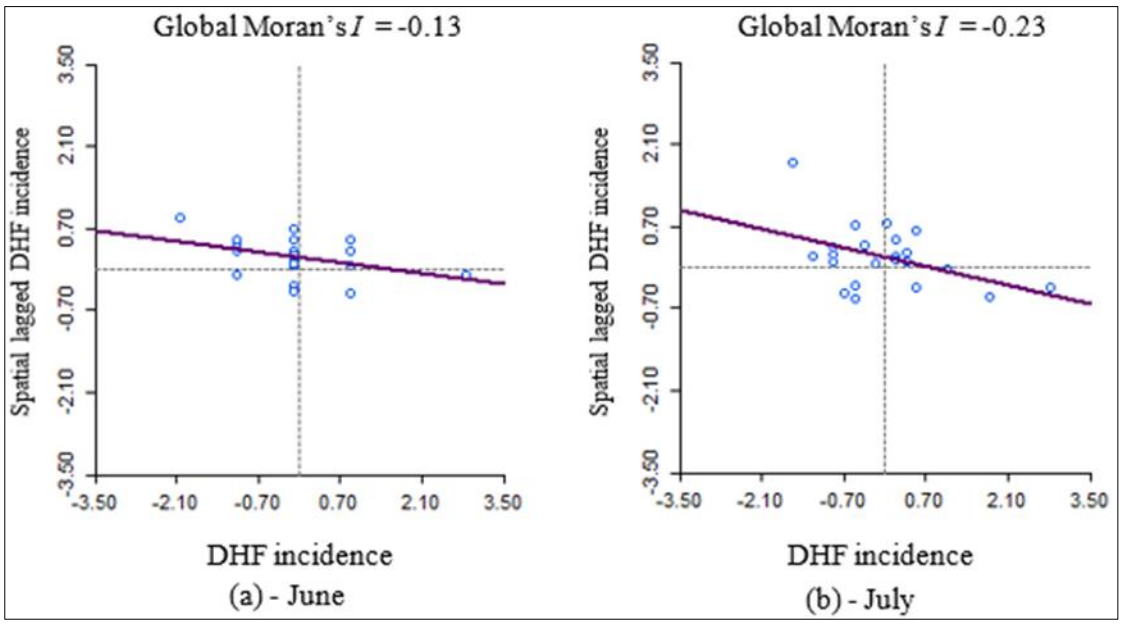

Figure 3 Moran's I scatterplots of DHF incidence

3.3. Analysis of spatio-temporal clustering of DHF

Data from boxplots in Figure 4 demonstrate the spatial distribution of local Moran's I coefficients collected in June and July. A statistical summary of their associated descriptive statistics may be found in Table 2. Table 1 presents data suggesting that there was negative geographical auto-correlation for DHF infection rates during these months, as indicated by the minimum values of the local Moran's I statistic. The local Moran's I median values, which ranged from -0.03 to -0.01, were nearly all centred at zero. June had the lowest value of the local Moran's I statistic throughout these two months, measuring -1.83. The maximum value of local Moran's I statistic was also detected in June with a value of 0.44. The values of the IQR and SDEV increased from June to July, according to measures of central tendency, with corresponding values falling into the ranges of [0.29; 0.34] and [0.44; 0.66], respectively. The data in Figure 4-a's

boxplots demonstrates how June's Moran's I index was comparatively uniformly distributed. This demonstrates that the distribution of the Moran's I value was quite even on either side of the -0.01 median. In the meantime, several of the Moan's I statistic's values were below mean values, as evidenced by the July Moran's I coefficients, which were skewed below the median.

Table 2 Statistical descriptives for local Moran's I statistic

Time periods	Statistical descriptives							
	Min	**Mean**	**Median**	**Max**	**Q1**	**Q3**	**IQR**	**SDEV**
June	-1.83	-0.12	-0.01	0.44	-0.25	0.03	0.29	0.44
July	-2.8	-0.22	-0.03	0.34	-0.23	0.09	0.33	0.66

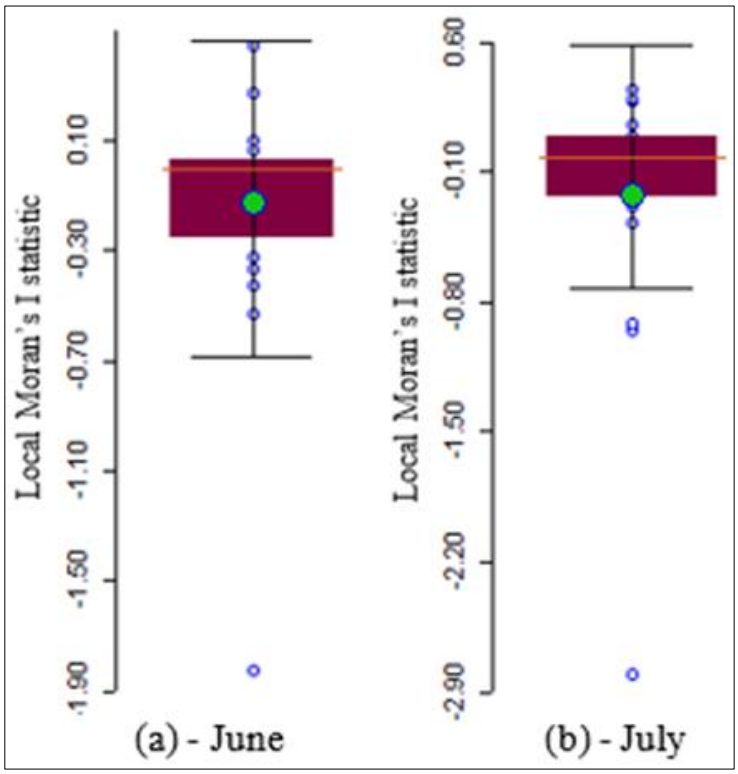

Figure 4 Local Moran's I statistic: (a) boxmap and (b) boxplot

According to data from the Boxmap (hinge = 1.5) in Figure 5, low Moran's I values were primarily found in the city's eastern and southern regions in June, while high Moran's I values were primarily found in the city's northern and western districts (Figure 5-a). In July, high values of the local Moran's I statistic were found in the western districts, but low values were also found in the southern districts.

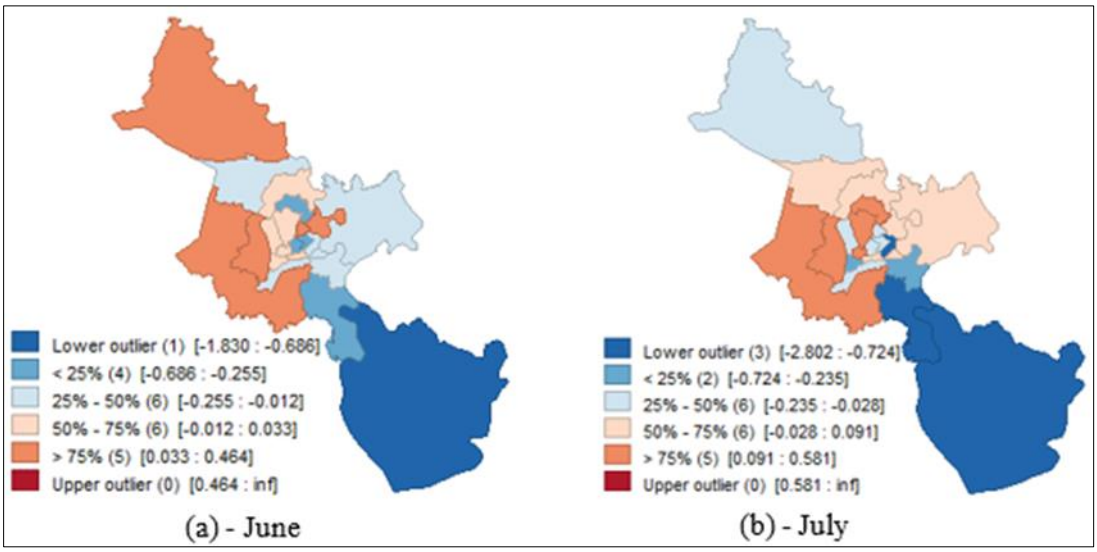

Figure 5 Boxmap of DHF incidence

Figure 6 displayed the spatial clusters of DHF incidence derived from the local Moran's I statistic. Spatial clusters were primarily found in the city centre, according to data from the local Moran's I cluster map, which is seen in Figure 4. In June 2023, only a low-high spatial cluster was located in the eastern part of the city, and statistically insignificant results were found in the 21 remaining districts (Figure 6-a). This indicates a distinctive change in the dynamics of spatial clusters from June to July. Although there were substantial DHF infection cases in some districts, including as District 1 (20 cases/100,000 people), Binh Chanh, and Binh Tan (12 cases/100,000 people), no spatial clusters were discovered in these locations. In the meantime, in July 2023, one low-high spatial anomaly cluster, one low-low spatial cluster, and one high-high spatial cluster were found. Nineteen districts were judged to be statistically insignificant at the 0.05 level during the month of July (Figure 6-b). As a result, the DHF spatial cluster migrated from the east towards the city centre as compared to those collected in June. District 4 (12 cases/100,000 people), Tan Binh (9 cases/100,000 people), and District 7 (9 cases/100,000 people) all had high-high, low-low spatial clusters as well as low-high spatial outliers. However, in districts with high infection rates, such District 1 (28 cases/100,000 people), Nha Be (22 cases/100,000 people), and District 8 (18 cases/100 people), no spatial clusters were found.

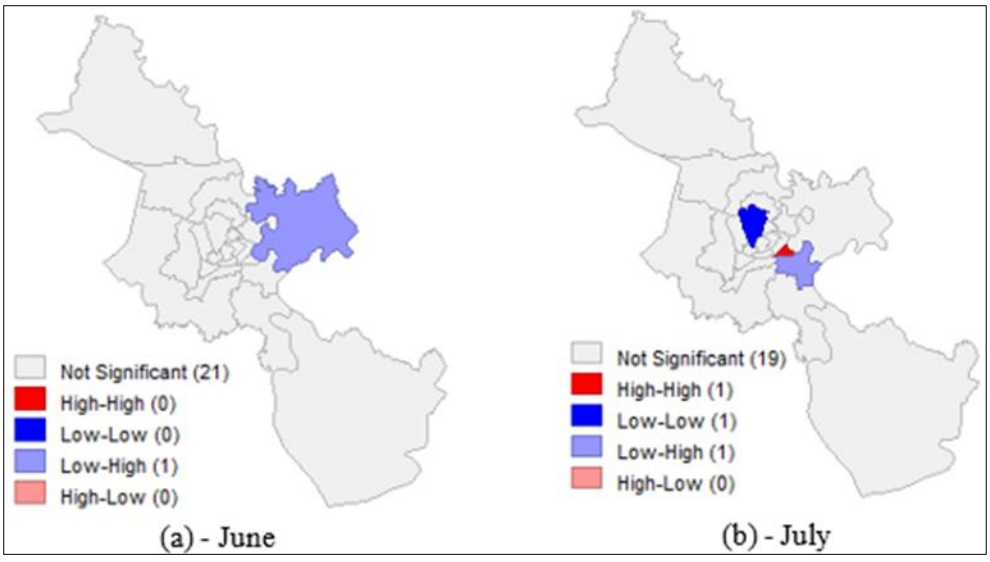

Figure 6 Local Moran's I cluster maps of dengue hemorrhagic fever incidence

The statistical significance levels for DHF infection rates from June to July in each district of Ho Chi Minh City in 2023 are displayed using data from significant maps in Figure 7. Four statistical levels were displayed: statistically significant at the 0.05, 0.01, and 0.001 levels, and statistically unsignificant (> 0.05). Data from Figure 7-a shows that, at the level

of 0.005, just one district was deemed to have statistical significance in June. Two districts were found in July at the 0.05 level of statistical significance. (Figure 7-b).

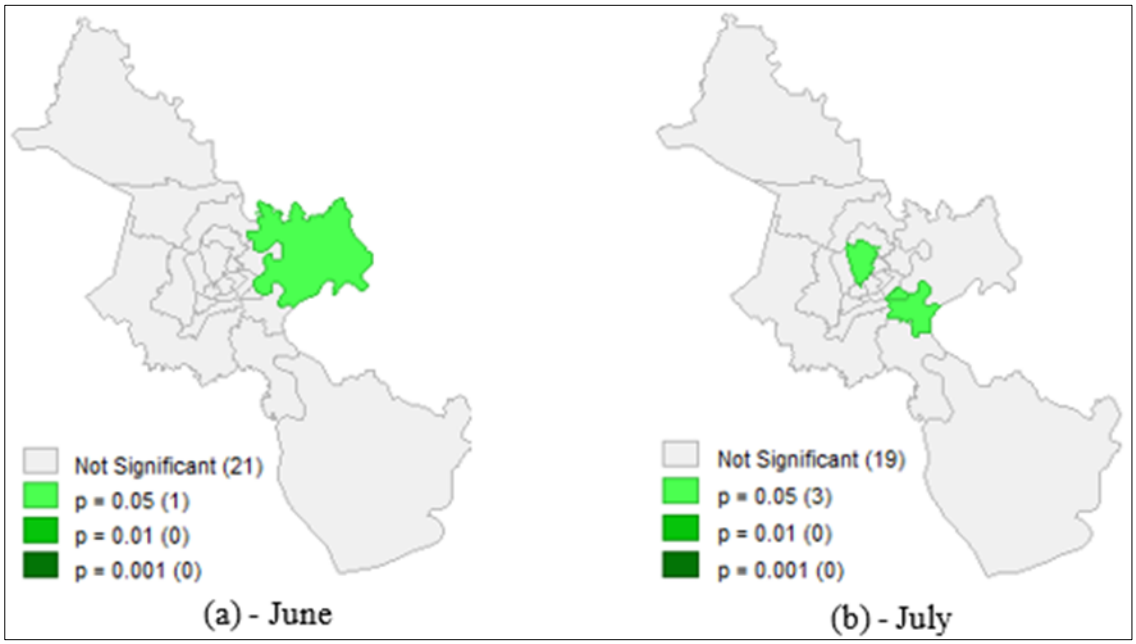

Figure 7 Significant maps of dengue hemorrhagic fever incidence

4. Conclusion

The goal of this study is to examine the spatial clustering of dengue hemorrhagic fever in Ho Chi Minh City, Vietnam, during the months of June through July of 2023. Initially, the data distribution was studied using descriptive statistics. The spatial clustering of dengue hemorrhagic fever over these four months was examined using the global Moran's I statistic, the Moran's I scatterplot, and the local Moran's I statistic. More specifically, using the local Moran's I statistic, dengue hemorrhagic fever clusters (high-high and low-low) and geographical outliers (low-high and high-low) were found in Ho Chi Minh City. In Ho Chi Minh City, it was discovered that DHF infection rates tend to rise gradually between June and July of 2023. High-high geographical clustering of DFH infection rates was primarily found in urban areas and the city centre, despite the fact that the spatial clustering of DHF infection rates has rapidly changed. The results of this investigation showed that Ho Chi Minh City has statistically significant spatial clusters of DHF. The findings of this investigation further show that local Moran's I statistic is validated in the context of studying the spatial clustering of infectious diseases in general and DHF in particular. The information gathered from this research will not only help us understand how DHF spreads better, but it can also significantly aid in the fight against dengue hemorrhagic fever.

Compliance with ethical standards

Acknowledgment

The authors would like to thank HCDC for providing the data. The authors acknowledge the editors and anonymous reviewers for their careful reading of our paper and their many insightful comments and suggestions.

Disclosure of conflict of interest

Authors declare that there is no conflict of interests.

Statement of informed consent

Informed consent was obtained from all individual participants included in the study

References

[1] Guzman MG, Kouri G. Dengue and dengue hemorrhagic fever in the Americas: lessons and challenges. J Clin Virol. 2003, 27(1):1–13.

[2] Mammen Jr MP, Pimgate C, Koenraadt CJM, Rothman AL, Aldstadt J, Nisalak A, et al. Spatial and temporal clustering of dengue virus transmission in Thai villages. PLoS Med. 2008, 5(11):e205.

[3] Wen T-H, Lin NH, Chao D-Y, Hwang K-P, Kan C-C, Lin KC-M, et al. Spatial–temporal patterns of dengue in areas at risk of dengue hemorrhagic fever in Kaohsiung, Taiwan, 2002. Int J Infect Dis. 2010, 14(4):e334–43.

[4] Wang W-H, Urbina AN, Chang MR, Assavalapsakul W, Lu P-L, Chen Y-H, et al. Dengue hemorrhagic fever–A systemic literature review of current perspectives on pathogenesis, prevention and control. J Microbiol Immunol Infect. 2020, 53(6):963–78.

[5] Kieu Q-L, Nguyen T-T, Hoang A-H. GIS and remote sensing: a review of applications to the study of the COVID-19 pandemic. Geogr Environ Sustain. 2021, 14(4).

[6] Gonzalez-Rubio J, Najera A, Arribas E. Comprehensive personal RF-EMF exposure map and its potential use in epidemiological studies. Environ Res. 2016, 149:105–12.

[7] Fecht D, Hansell AL, Morley D, Dajnak D, Vienneau D, Beevers S, et al. Spatial and temporal associations of road traffic noise and air pollution in London: Implications for epidemiological studies. Environ Int. 2016, 88:235–42.

[8] Alves JD, Abade AS, Peres WP, Borges JE, Santos SM, Scholze AR. Impact of COVID-19 on the indigenous population of Brazil: A geo-epidemiological study. Epidemiol Infect. 2021, 149:e185.

[9] Şener R, Türk T. Spatiotemporal analysis of cardiovascular disease mortality with geographical information systems. Appl Spat Anal Policy. 2021, 14(4):929–45.

[10] Xie Z, Qin Y, Li Y, Shen W, Zheng Z, Liu S. Spatial and temporal differentiation of COVID-19 epidemic spread in mainland China and its influencing factors. Sci Total Environ. 2020, 744:140929.

[11] Aral N, Bakır H. Spatiotemporal pattern of Covid-19 outbreak in Turkey. GeoJournal. 2023, 88(2):1305–16.

[12] Zhang P, Yang S, Dai S, Aik DHJ, Yang S, Jia P. Global spreading of Omicron variant of COVID-19. Geospat Health. 2022, 17(s1).

[13] Nguyen HX, Chu C, Nguyen HLT, Nguyen HT, Do CM, Rutherford S, et al. Temporal and spatial analysis of hand, foot, and mouth disease in relation to climate factors: a study in the Mekong Delta region, Vietnam. Sci Total Environ. 2017, 581:766–72.

[14] Deng T, Huang Y, Yu S, Gu J, Huang C, Xiao G, et al. Spatial-temporal clusters and risk factors of hand, foot, and mouth disease at the district level in Guangdong Province, China. PLoS One. 2013, 8(2):e56943.

[15] Shariati M, Mesgari T, Kasraee M, Jahangiri-Rad M. Spatiotemporal analysis and hotspots detection of COVID-19 using geographic information system (March and April, 2020). J Environ Heal Sci Eng. 2020, 18:1499–507.

[16] Al-Kindi KM, Alkharusi A, Alshukaili D, Al Nasiri N, Al-Awadhi T, Charabi Y, et al. Spatiotemporal assessment of COVID-19 spread over Oman using GIS techniques. Earth Syst Environ. 2020, 4:797–811.

[17] Samphutthanon R, Kumar Tripathi N, Ninsawat S, Duboz R. Spatio-temporal distribution and hotspots of hand, foot and mouth disease (HFMD) in northern Thailand. Int J Environ Res Public Health. 2014, 11(1):312–36.

[18] Xiao G, Hu Y, Ma JQ, Hao YT, Wang XF, Zhang YJ, et al. Spatial clustering and changing trend of hand-foot-mouth disease during 2008-2011 in China. Zhonghua liu xing bing xue za zhi= Zhonghua liuxingbingxue zazhi. 2012, 33(8):808–12.

[19] Xu L, Shi Y, Rainey JJ, Zhang Z, Zhang H, Zhao J, et al. Epidemiological features and spatial clusters of hand, foot, and mouth disease in Qinghai Province, China, 2009–2015. BMC Infect Dis. 2018, 18(1):1–11.

[20] Wang C, Li X, Zhang Y, Xu Q, Huang F, Cao K, et al. Spatiotemporal cluster patterns of hand, foot, and mouth disease at the county level in mainland China, 2008-2012. PLoS One. 2016, 11(1):e0147532.

[21] Cattarino L, Rodriguez-Barraquer I, Imai N, Cummings DAT, Ferguson NM. Mapping global variation in dengue transmission intensity. Sci Transl Med. 2020, 12(528):eaax4144.

[22] Ty Hang VT, Holmes EC, Veasna D, Quy NT, Tinh Hien T, Quail M, et al. Emergence of the Asian 1 genotype of dengue virus serotype 2 in viet nam: in vivo fitness advantage and lineage replacement in South-East Asia. PLoS Negl Trop Dis. 2010, 4(7):e757.

[23] Tran VT, Inward RPD, Gutierrez B, Nguyen NM, Rajendiran I, Thanh PN, et al. Cryptic transmission and re-emergence of Cosmopolitan genotype of Dengue Virus Serotype 2 within Ho Chi Minh City and Southern Vietnam. medRxiv. 2023, 2004–23.

[24] Fisher MJ, Marshall AP. Understanding descriptive statistics. Aust Crit care. 2009, 22(2):93–7.

[25] Kaur P, Stoltzfus J, Yellapu V. Descriptive statistics. Int J Acad Med. 2018, 4(1):60–3.

[26] Phinyomark A, Thongpanja S, Hu H, Phukpattaranont P, Limsakul C. The usefulness of mean and median frequencies in electromyography analysis. Comput Intell Electromyogr Anal Perspect Curr Appl Futur challenges. 2012, 23:195–220.

[27] Rodbard D. Glucose time in range, time above range, and time below range depend on mean or median glucose or HbA1c, glucose coefficient of variation, and shape of the glucose distribution. Diabetes Technol Ther. 2020, 22(7):492–500.

[28] Cliff AD, Ord JK. Spatial processes: models & applications. (No Title). 1981,

[29] Getis A, Ord JK. Local spatial statistics: An overview. Spatial analysis: Modeling in a GIS environment. Longley, P., and M. Batty. Wiley, New York, 1996.

[30] Vu D-T, Nguyen T-T, Hoang A-H. Spatial clustering analysis of the COVID-19 pandemic: A case study of the fourth wave in Vietnam. Geogr Environ Sustain. 2021, 14(4).

[31] Nguyen TT, Vu TD. Identification of multivariate geochemical anomalies using spatial autocorrelation analysis and robust statistics. Ore Geol Rev. 2019, 111.

[32] Anselin L. Local indicators of spatial association—LISA. Geogr Anal. 1995, 27(2):93–115.